

## Semiclassical computations of time-dependent tunneling

M. Kira, I. Tittonen, W. K. Lai, and S. Stenholm

*Research Institute for Theoretical Physics, P.O. Box 9, FIN-00014 University of Helsinki, Finland*

(Received 5 July 1994; revised manuscript received 1 November 1994)

In this paper we consider the time evolution of wave-packet tunneling through a potential barrier. Using a path-summation approach, we can describe the quantum evolution in terms of particle trajectories both in the allowed and forbidden regions. Near the barrier edges, where the potential changes rapidly, the wave aspects dominate. These make the trajectories branch into infinite families of paths, which have to be included in the summation. Combining these features, we treat correctly the complementary aspects of the full quantum process, and this allows us to obtain a computational method that gives accurate numerical results with considerably less expenditure of computer time than a direct integration of the Schrödinger equation. We test the method on a simple rectangular potential by comparing the calculations with both conventional wave scattering results and computations from the Schrödinger equation. A general potential can be approximated by a staircase, which allows the application of our method. A simple adiabatic extension is shown to work excellently for the case of a periodically modulated barrier.

PACS number(s): 31.70.Hq, 03.65.Sq, 73.40.Gk

### I. INTRODUCTION

It was early recognized that tunneling is one of the most remarkable nonclassical manifestations of quantum dynamics, and it is an essential feature of many physical phenomena. It makes a contribution to various chemical reactions, and its use in electronic devices goes back to the Esaki diode of the 1960s. Modern semiconductor technology manufactures heterostructures, where the dynamics of charge carriers is dominated by quantum features; for a recent review see Ref. [1].

The customary approach to tunneling (see, e.g., Ref. [2]) is to calculate the stationary states and compare their strength on one side of the barrier with that penetrating to the other side. The transmission probability can be obtained in a fair approximation using the semiclassical WKB approach [2]. A particularly popular method continues classical variables like time and momentum into the complex plane. This has been used in condensed-matter theory, phase-transition problems, reaction rate calculations, and cosmological problems; for reviews and many references consult, e.g., Ref. [3]. The tunneling decay rate has been calculated in terms of an imaginary-time propagator; see Coleman's review [4]. This approach allowed Caldeira and Legget [5] to add dissipative features to quantum tunneling. However, all these investigations are fundamentally time-independent Schrödinger equation calculations. Recently the development of well-controlled femtosecond laser pulses has made it possible to interrogate quantum dynamics in real time. In addition to the fundamental task of verifying the Schrödinger equation in the time domain, this technology has become an efficient tool in many areas of applications; see the articles in Ref. [6]. These developments motivate a discussion of time-dependent quantum phenomena and wave-packet propagation. Except for purely pedagogical examples (see, e.g., Ref. [2]), only a few in-

vestigations have explicitly considered the time evolution of quantum tunneling. Semiconductor device applications have initiated a discussion of tunneling times [7,8]. In such applications, temporal variation of the structural parameters has been considered in several papers [9–13]. In these cases the computation of electronic wave-packet propagation has provided a valuable complement to scattering calculations.

The semiclassical approximation makes it possible to describe quantum evolution in terms of the action function calculated from classical trajectories [14]. This approach has been extended to complex time integration by Miller and George [15–17]. In [18] they explicitly display the tunneling trajectories allowing penetration into classically forbidden regions. It is the purpose of this paper to utilize semiclassical understanding to calculate the time-dependent aspects of a wave packet penetrating potential barriers.

Wave packets can be propagated exactly when the Green function of the time-dependent Schrödinger equation is known. This can be expressed in terms of Feynman path integrals [3]. However, even the simple case of rectangular potential barriers has been solved exactly only recently [19,20]. The results are complicated, and only of limited use in numerical applications. Needless to say, any additional complications make exact solutions unavailable.

In the case of a rectangular barrier like Fig. 1, or potentials very close to this, we can divide the space into external and internal regions. Far from the barrier, the particle is free and the semiclassical propagator is exact. Here we can, consequently, interpret the propagator entirely in terms of particle paths. Classically these turn around when they encounter the barrier, but the wave mechanical nature of the system allows barrier penetration, making the particles emerge in the classically allowed region on the other side of the barrier. There

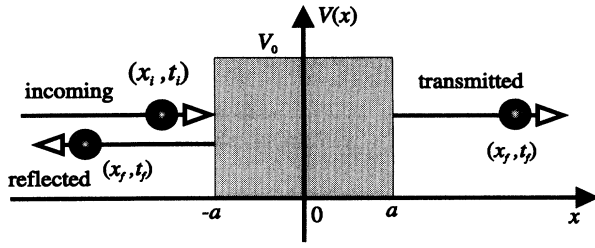


FIG. 1. In this picture a particle, represented by a sphere, is reflected or transmitted from a rectangular barrier. The particle is initially at  $(x_i, t_i)$  and finally at  $(x_f, t_f)$ .

again a classical path description holds. Thus the propagation can be described in terms of classical mechanics everywhere except during the tunneling, where wave mechanics prevails; the phenomenon is an illustration of complementarity in quantum mechanics. It is the aim of the present paper to utilize this freedom to use a complementary description to obtain a computationally accurate and intuitively transparent approach to tunneling.

To this end we calculate classical paths outside the barrier. These are the stationary phase solutions to the path integrals. Following Miller and George, we convert to an imaginary-time description inside the barrier, when the paths correspond to a steepest descent approach. In areas of constant potential, these give an exact quantum description inside the barrier. The wave features of the particles manifest themselves only near the barrier edges, where the potential varies rapidly. Here we can define reflection and transmission coefficients as in classical wave physics, and these split up any incoming particle path into reflected and transmitted components. In the classical path description each trajectory encountering the boundary branches into two separate ones, with their ratio given by wave mechanics. Thus we obtain an infinite multitude of semiclassical trajectories, each of which contributes to the action giving the wave function of the system. The quantum features are seen in the possibilities of interference between the waves deriving from each semiclassical trajectory.

We have also written a numerical program to calculate the time-dependent evolution of a wave packet using the one-dimensional Schrödinger equation; see Ref. [21]. The time steps are implemented using a split-operator method. The program can be applied to both molecular energy levels and semiconductor heterostructures by the use of an appropriate scaling. We introduce time and space scales  $T_c$  and  $R_c$ , respectively. In addition, we choose the energy scale  $V_0 = 0.5$  eV as being relevant both for molecular vibrations and semiconductor potential differences. This fixes the time scale to be  $T_c = \hbar/V_0 = 1.316$  fs. This is in a suitable range for the dynamic phenomena investigated by short pulse lasers. The space scale depends on the mass according to  $R_c = (\hbar T_c / 2m)^{1/2}$ . In GaAs the effective mass is 7% of the free-electron mass giving  $R_c = 1.04$  nm; for a molecular mass of 20 proton masses, we find  $R_c = 0.0144$  Å. In both cases the relevant dimensionless space variable extends to about 100 times the basic unit  $R_c$ . It is thus pos-

sible to adapt the numerical integration method of Ref. [21] to deal with both parameter ranges. All results presented in this paper have been verified by numerical computation from the time-dependent Schrödinger equation.

This paper presents results as follows. The time-dependent propagator is introduced in Sec. II. Section III describes its calculation in terms of classical trajectories penetrating into the tunneling region. Section IV shows how the wave aspect splits the trajectories at the potential edges. These complementary aspects are combined in Sec. V to give a full semiclassical description of time-dependent tunneling phenomena. In Sec. VI we discuss the extension of the method beyond the case of rectangular and stationary potential barriers. The computational applications of the trajectory method are presented in Sec. VII and compared with the quantum-dynamical evolution of wave packets obtained by exact numerical evaluation of the time-dependent Schrödinger equation. To justify our choice of a rectangular potential, we have used parameters relevant to the physics of semiconductor heterostructures. Finally, in Sec. VII we present the conclusions of the work.

## II. THE PROPAGATOR AS A SUM OVER PATHS

In quantum mechanics the wave function at the time  $t_f$  can be obtained from the wave function at an earlier time  $t_i$  by a linear kernel according to

$$\Psi(x_f, t_f) = \int K(x_f, t_f | x_i, t_i) \Psi(x_i, t_i) dx_i, \quad (1)$$

where the final coordinate is denoted by  $x_f$ . The integral kernel  $K$  is the Green function of the nonrelativistic Schrödinger equation. According to Feynman [22], this can be represented by the functional integral

$$K_{fi} = K(x_f, t_f | x_i, t_i) = \int \mathcal{D}x e^{iS_{fi}/\hbar}, \quad (2)$$

where the integration goes over all paths from  $(x_i, t_i)$  to  $(x_f, t_f)$  with the appropriate measure. The function in the exponent is the expression for the classical action

$$S_{fi} = \int_{t_i}^{t_f} L(\dot{x}, x) dt = \int_{t_i}^{t_f} [\frac{1}{2} m \dot{x}^2 - V(x)] dt. \quad (3)$$

Using the stationary phase approximation, we obtain the maximal contribution from those paths in expression (2) which are determined such that the variation around them is zero ( $\delta S = 0$ ). These paths are determined by the classical equation of motion. If there is more than one classical path leading from  $x_i$  to  $x_f$  in the time interval  $[t_i, t_f]$ , we may write the propagator (2) in the form

$$K_{fi} = \sum_n e^{iS^{(n)}/\hbar} \int \mathcal{D}\eta e^{i\tilde{S}^{(n)}(\dot{\eta}, \eta, x_{cl})/\hbar}, \quad (4)$$

where the sum  $n$  goes over all such paths. The terms in expression (4) consist of actions along the classical paths and quantum correction path integrals in the neighborhood of these paths. Expression (4) is a truly semiclassical expression; the paths involved are determined from the classical equations of motion, but applying the propagator (4) in Eq. (1) allows interference between various

paths, which is a genuinely wave mechanical feature. We now proceed to consider these two aspects in some detail.

III. THE PARTICLE ASPECT OF TUNNELING

The trajectories leading to a stationary phase in the path integral are given by the Lagrange equation of motion. It is well known that this admits the constant of motion

$$E = \frac{1}{2}m\dot{x}^2 + V(x). \tag{5}$$

Solving this for the time dependence, we obtain

$$t - t_i = \int_{x_i}^x \frac{dx'}{\sqrt{2[E - V(x')]/m}}, \tag{6}$$

compare Refs. [23] and [24]. We are now going to make a formal generalization of the path concept into classically forbidden regions. We thus consider a part of space with  $V(x) > E$ , where no classical trajectories can penetrate. However, formally the integral expression (6) can be continued into such regions of  $x$  when we allow  $t$  to become a complex variable. Hence the equation of motion is continued from the real  $t$  axis into the complex plane in a manner well known from the theory of ordinary differential equations. This type of integration has been extensively used by Miller and George in several applications [15,18].

In order to carry out the following investigations explicitly, we consider the simple rectangular potential barrier shown in Fig. 1. We assume that the particle enters with the initial velocity  $v_i$  at  $(x_i, t_i)$ , and that its total energy is

$$E = \frac{1}{2}mv_i^2. \tag{7}$$

The particle reaches the barrier at  $x = -a$  at time  $t_-$ , and we write the integrated time from Eq. (6) for  $x < a$  in the form

$$t - t_i = \int_{t_i}^{t_-} dt + \int_{-a}^x \frac{dx'}{\sqrt{v_i^2 - 2V_0/m}} = t_- - t_i \pm i \frac{x+a}{w} \tag{8}$$

where

$$w^2 = 2V_0/m - v_i^2. \tag{9}$$

If we set  $x = +a$ , we find that the trajectory emerges on the other side of the barrier at the time

$$t = t_- \pm i\tau. \tag{10}$$

The final time can be obtained from the final position  $x_f > a$  as

$$t(x_f) = t_- \pm i\tau + \int_a^{x_f} \frac{dx}{v_i} = t_- \pm i\tau + (t_f - t_-) = t_f \pm i\tau. \tag{11}$$

From this we can see that the traversal through the classically excluded region has added the imaginary part  $\pm i\tau$  to the time used to get from  $x_i$  to  $x_f$ .

In order to fix the sign of the imaginary part, we consider the action in the excluded region,

$$\begin{aligned} \frac{i}{\hbar} \int [\frac{1}{2}m\dot{x}^2 - V_0] dt &= -\frac{i}{\hbar} \int \left[ \frac{1}{2}m \left( \frac{dx}{d\tau} \right)^2 + V_0 \right] (\pm i d\tau) \\ &= \pm \frac{1}{\hbar} \int \mathcal{H} \left[ m \frac{dx}{d\tau}, x \right] d\tau, \end{aligned} \tag{12}$$

where  $\mathcal{H}$  is formally the Hamiltonian of the system. In order to make large energies  $\mathcal{H}$  damp out, we have to choose the time evolution in the direction of the negative imaginary axis  $-i\tau$ . We choose this branch in the following. Now the stationary phase method becomes the method of steepest descent. The paths we use for tunneling are such that the difference between the initial and final positions is given by  $t(x_f) - t(x_i) = t_{\text{fl}} - i\tau$ . We define the modified propagator by the formal expression

$$\begin{aligned} \tilde{K}(x_f, x_i, t_{\text{fl}}) &= \int \mathcal{D}x \exp \left\{ \frac{i}{\hbar} \left[ \int_{t_i}^{t_-} L dt + \int_{t_-}^{t_- - i\tau} L dt \right. \right. \\ &\quad \left. \left. + \int_{t_- - i\tau}^{t_f - i\tau} L dt \right] \right\}. \end{aligned} \tag{13}$$

We want to point out that the original propagator (2) does not have any classical path solutions: the time evolution has to be modified as in Eq. (13). The time path chosen for the integration is shown in Fig. 2. During part *A* the path  $x_{cl}$  propagates from  $x_i$  to  $-a$ , in part *B* it propagates from  $-a$  to  $a$ , and in part *C* from  $a$  to  $x_f$ . This is reached at the unphysical time  $t_f - i\tau$ . To obtain the physically applicable propagator we consider  $\tilde{K}(x_f, x_i, t_{\text{fl}})$  in Eq. (13) as an analytic function of the variable  $t_{\text{fl}}$  and carry out an analytic continuation to the real-time axis by the replacement  $t_{\text{fl}} \rightarrow t_{\text{fl}} + i\tau$ . In order to obtain the classical paths, we integrate the equation of motion separately in the three regions of Fig. 2. As we have no forces acting inside the regions, we obtain the expressions

$$x(t) = \begin{cases} v_i(t - t_-) - a, & x \leq -a \end{cases} \tag{14a}$$

$$x(t) = \begin{cases} iw(t - t_-) - a, & -a < x < a \end{cases} \tag{14b}$$

$$x(t) = \begin{cases} v_i(t - t_- + i\tau) + a, & x > a. \end{cases} \tag{14c}$$

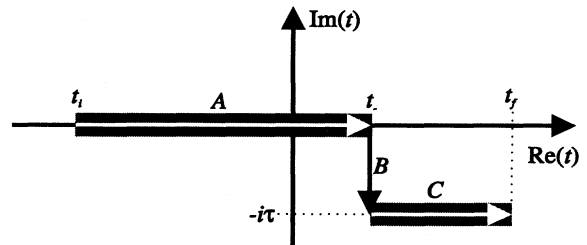


FIG. 2. This picture illustrates how the integration is performed in Eq. (13). The time evolution is divided into three parts *A*, *B*, and *C*.

Choosing

$$\tau = \frac{2a}{w}, \quad (15)$$

we obtain a continuous path in Eqs. (14). Choice (15) is in full agreement with the general expression in Eq. (11). Writing out the expression for  $x(t_i)$  and  $x(t_f - i\tau)$  from Eq. (14), we can express the initial velocity in terms of traveled distance  $x_{fi}$  and elapsed physical time as

$$\begin{aligned} x_i &= x(t_i) = v_i(t_i - t_-) - a, \\ x_f &= x(t_f - i\tau) = v_i(t_f - t_-) + a. \end{aligned} \quad (16)$$

From this the velocity  $v_i$  is obtained as

$$v_i = \frac{|x_f| - x_i - 2a}{t_{fi}}. \quad (17)$$

Here we have taken the absolute value of  $x_f$  in order to obtain the correct expression even when the path is reflected from the barrier (Fig. 1). The observed travel time  $t_{fi}$  from  $x_i$  to  $x_f$  follows from the velocity  $v_i$  in such a way that no time appears to be consumed by the tunneling through the potential. In a separate publication we will discuss the semiclassical interpretation of tunneling times.

#### IV. THE WAVE ASPECT OF TUNNELING

The quantum tunneling cannot be described entirely in terms of classical paths even when complex time is introduced. Expression (4) includes quantum interference between different equivalent paths leading to the same final coordinates  $(x_f, t_f)$ . In the present case, these arise because for matter waves each interface acts as a beam splitter, making the path branch into two additional ones after each encounter with the interface. This is a pure wave property well known from classical optics. In order to obtain a full description of quantum tunneling, we must include this feature properly. First of all we have to match the wave functions at the boundary. For each term in series (4) we have an expression of the form

$$K_{fi}^{(n)} = e^{iS_{cl}^{(n)}/\hbar} A^{(n)}. \quad (18)$$

In Fig. 3 we show a situation where the incoming wave function  $\Psi_i$  impinges on the boundary between regions I and II. (Note that now  $x_f$  is near the interface at  $x_0$ .) This is divided into a reflected wave  $\Psi_r$  and a transmitted one  $\Psi_t$ . Both the wave function and its derivative have to be continuous at the boundary. Because the wave functions according to Eq. (1) are proportional to the propagators  $K$ , at the boundary we find

$$K_i + K_r = K_t, \quad (19a)$$

$$\frac{\partial K_i}{\partial x} + \frac{\partial K_r}{\partial x} = \frac{\partial K_t}{\partial x}. \quad (19b)$$

We will argue in Appendix A that the derivative of the amplitude  $A^{(n)}$  can be neglected for large enough  $t_{fi}$ , and hence we obtain

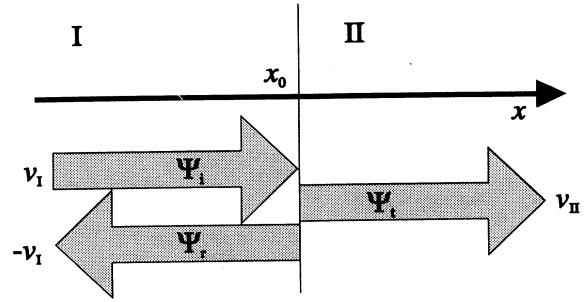


FIG. 3. A wave function encounters a boundary at  $x_0$ . Region I contains the incoming and reflected wave functions, and region II the transmitted wave function.

$$\left[ \frac{\partial K}{\partial x_f} \right]_{x_f=x_0} = \frac{i}{\hbar} \left[ \frac{\partial S_{cl}^{(n)}}{\partial x_f} K \right]_{x_f=x_0} = \left[ \frac{imv_f}{\hbar} K \right]_{x_f=x_0}, \quad (20)$$

where the classical action relation  $\partial S_{cl}/\partial x_f = p_f$  has been used. Here  $v_f$  is the velocity at the end of the classical path. With the notation of Fig. 3, relation (19b) becomes

$$v_I(A_i - A_r) = v_{II}A_t \quad (21)$$

because  $S_{cl}$  has the same value for all waves at the surface  $x_f = x_0$ . From (21) and (19a) we obtain the reflection and transmission coefficients

$$R = \frac{A_r}{A_i} = \frac{v_I - v_{II}}{v_I + v_{II}}, \quad (22)$$

$$T = \frac{A_t}{A_i} = \frac{2v_I}{v_I + v_{II}}. \quad (23)$$

These are similar to corresponding coefficients for electromagnetic waves [25].

The transmission and reflection coefficients can be generalized to the potential barrier using the imaginary time argument. We use the notation defined in Fig. 4. Inside the barrier we have  $v = iw$ , and directly obtain

$$T_- = \frac{2v_i}{v_i + iw}, \quad R_- = \frac{v_i - iw}{v_i + iw}, \quad (24)$$

$$T_+ = \frac{2iw}{v_i + iw}, \quad R_+ = \frac{iw - v_i}{v_i + iw} = -R_-. \quad (25)$$

The coefficients  $\tilde{T}_+$  and  $\tilde{R}_+$  (Fig. 4) are obtained by time or space inversion and, because all coefficients are symmetric with respect to time inversion, we have

$$\tilde{T}_+ = T_+, \quad \tilde{R}_+ = R_+. \quad (26)$$

For further use we note the normalization of the determinant

$$\det \begin{bmatrix} T_- & R_- \\ R_+ & T_+ \end{bmatrix} = T_- T_+ - R_- R_+ = 1. \quad (27)$$

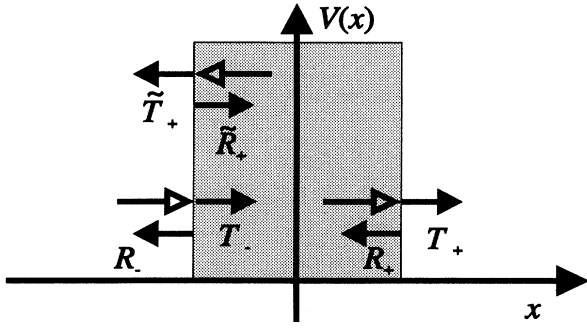


FIG. 4. A particle path can approach the barrier in three different ways. Each implies different transmission and reflection coefficients.

### V. SEMICLASSICAL DESCRIPTION OF QUANTUM TUNNELING

We are now going to combine the wave properties of Sec. IV at interfaces with the particle trajectory approach of Sec. III. According to Fig. 5 each trajectory splits in two every time it encounters the potential edge, thus proliferating the trajectories into an infinite family consisting of all possible cases of reflections back and forth inside the barrier. Each case provides its own contribution to the sum in Eq. (4), and the reflected (transmitted) propagator is made up of the sum of all even (odd) traverses of the interior of the barrier. We need to evaluate the contribution to the action from each such path and insert this into the place of the classical action (4). When the imaginary-time contributions are included, this will be called the semiclassical action  $\tilde{S}_{fi}$ . From Eq. (13) we directly obtain

$$\begin{aligned} \tilde{S}_{fi} &= \int_{t_i}^{t_-} L dt + \int_{t_-}^{t_- + i\tau} L dt + \int_{t_- + i\tau}^{t_f - i\tau} L dt \\ &= \frac{1}{2}mv_i^2(t_- - t_i) + (\frac{1}{2}mw^2 + V_0)i\tau + \frac{1}{2}mv_i^2(t_f - t_-). \end{aligned} \quad (28)$$

We use the formal energy conservation (9) to eliminate the potential parameter  $V_0$  and obtain

$$\tilde{S}_{fi} = \frac{1}{2}mv_i^2(t_{\tilde{f}} + i\tau) + imw^2\tau. \quad (29)$$

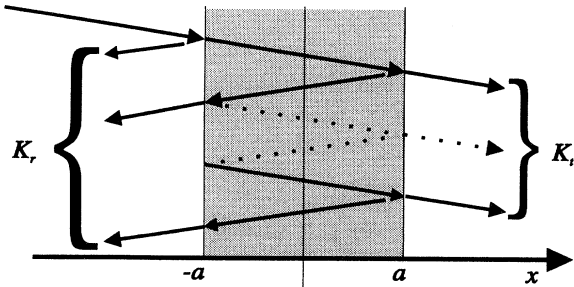


FIG. 5. Schematic picture illustrating the construction of transmission and reflection propagators.

For a path traversing the interior of the barrier  $n$  times, from Eq. (15) we obtain the expression

$$\tau = \frac{2a}{w}n, \quad (30)$$

and  $v_i$  should be regarded as a function of  $x_{\tilde{f}}$  and  $t_{\tilde{f}}$  according to Eq. (17). The replacement  $t_f \rightarrow t_f + i\tau$  has to be made in the action  $\tilde{S}_{\tilde{f}}$  in order to produce the physically relevant propagator, and from (29) we obtain

$$\begin{aligned} \tilde{S}_{\tilde{f}}(t_{\tilde{f}} \rightarrow t_{\tilde{f}} + i\tau) &= \frac{m(x_{\tilde{f}} - 2a)^2}{2(t_{\tilde{f}} + i\tau)^2} (t_{\tilde{f}} + 2i\tau) \\ &\quad + 2iamn \left[ \frac{2V_0}{m} - \left( \frac{x_{\tilde{f}} - 2a}{t_{\tilde{f}} + i\tau} \right)^2 \right]^{1/2} \\ &= \frac{1}{2}mv_i^2 t_{\tilde{f}} + 2iamwn - \frac{1}{2}mv_i^2 t_{\tilde{f}} \left( \frac{\tau}{t_{\tilde{f}}} \right)^2 \\ &\quad + \mathcal{O} \left( \frac{\tau}{t_{\tilde{f}}} \right)^3. \end{aligned} \quad (31)$$

In the limit when

$$t_{\tilde{f}} \gg \tau, \quad (32)$$

we can replace the action by the first two terms in (31), which only implies that we consider the transfer of the state over times much longer than the parameter (15). When we now calculate the contribution to the propagator  $K_{fi}$  from a path with  $n$  traverses inside the barrier, we assign to it the action given by just the first two terms of (31).

In the regions  $|x| > a$ , the particle propagates freely, and the classical action is known to give an exact expression for the quantum propagator

$$K_{cl} = \left( \frac{m}{2\pi i \hbar t_{\tilde{f}}} \right)^{1/2} e^{imv_i^2 t_{\tilde{f}} / 2\hbar}. \quad (33)$$

This contributes to each path between any points  $x_i$  and  $x_f$  as can be seen from Eq. (31).

We are now in the position to add up all the semiclassical paths leading to the transmitted and reflected propagators in Fig. 5. Each one will contain a factor  $K_{cl}$  given by the free propagator (33).

We start by following all the paths in Fig. 5 leading to the transmission propagator  $K_+$ . Each reflection or transmission should be described by the appropriate coefficient according to Fig. 4. To each path we assign a phase given by  $i/\hbar$  times its contribution to the semiclassical action from Eq. (31).

The result of all semiclassical paths is

$$\begin{aligned} K_+ &= K_{cl} T_- e^{-2amw/\hbar} \sum_{n=0}^{\infty} R_+^{2n} e^{-n4amw/\hbar} T_+ \\ &= K_{cl} \frac{T_- T_+}{e^{2amw/\hbar} - R_+^2 e^{-2amw/\hbar}} \equiv K_{cl} \mathcal{T}, \end{aligned} \quad (34)$$

where the geometric series has been summed. The factor  $\mathcal{T}$  is the transmission coefficient for the potential barrier.

We obtain the reflection propagator in the same way:

$$\begin{aligned}
K_r &= K_{cl} \left[ R_- + T_- e^{-4amw/\hbar} R_+ + T_+ \sum_{n=0}^{\infty} R_+^{2n} e^{-n4amw/\hbar} \right] \\
&= K_{cl} \frac{R_- + R_+ (T_- T_+ - R_- R_+) e^{-4amw/\hbar}}{1 - R_+^2 e^{-4amw/\hbar}} \\
&= K_{cl} R_- \frac{e^{2amw/\hbar} - e^{-2amw/\hbar}}{e^{2amw/\hbar} - R_+^2 e^{-2amw/\hbar}} \equiv K_{cl} \mathcal{R}, \quad (35)
\end{aligned}$$

where relations (25) and (27) have been used.  $\mathcal{R}$  is the total reflection coefficient of the barrier. When we combine all the contributions to the full propagator  $K_{fi}$ , we must also consider the fact that, when  $x_f \leq -a$ , there is the possibility of direct propagation from  $x_i$  to  $x_f$  without ever entering the barrier. We denote this propagator by  $K_{cl}^d$ . We note that the velocity in Eq. (33) is to be defined here as

$$v_i^d = \frac{|x_f - x_i|}{t_{fi}}. \quad (36)$$

The total propagator is then given by the expression

$$\begin{aligned}
K(x_f, t_f | x_i, t_i) \\
= (K_{cl}^d + K_{cl} \mathcal{R}) \Theta(-a - x_f) + K_{cl} \mathcal{T} \Theta(x_f - a). \quad (37)
\end{aligned}$$

When this expression is applied to an initial monochromatic plane-wave state, the ordinary scattering representation

$$\begin{aligned}
\Psi(x, t) = \{ [e^{ikx} + \mathcal{R}(\hbar k/m) e^{-ik2a} e^{-ikx}] \Theta(-a - x) \\
+ \mathcal{T}(\hbar k/m) e^{-ik2a} e^{ikx} \Theta(x - a) \} e^{-iE_k t/\hbar} \quad (38)
\end{aligned}$$

follows.

In order to obtain information about the tunneling process we need not include the contributions inside the barrier,  $|x| < a$ , into the propagator (37). The relevant information was utilized in calculating the coefficients  $\mathcal{R}$  and  $\mathcal{T}$ . As no observation is going to be made inside the barrier, the propagator is not needed in this region. However, it can be constructed from our results in a straightforward way.

The semiclassical result in Eq. (37) adds contributions from the paths in a coherent way. This allows for interference between the wave functions generated by all paths. We consider the case of tunneling here, hence the trajectories traversing back and forth inside the barrier all derive from imaginary-time dynamics. If the energy is above the barrier, the stationary phase approximation of Eq. (2) gives only one classical path which passes over the barrier. However, the wave nature of the particles will, even in this case, give reflections at the interfaces and cause a proliferation of the trajectories into many single ones which can interfere. Only when this effect is included in the semiclassical calculation can we obtain agreement with the wave mechanical description. If we include only the allowed classical trajectory from  $x_i$  to  $x_f$ , all quantum interferences are lost.

For overbarrier transmission the velocity in the region  $|x| < a$  becomes real, and the time can be kept real. This means that its action enters into sums of the type (34) and

(35) as a genuine phase factor. The resulting expressions become rapidly oscillating and do not have the excellent convergence properties of the tunneling case. Nevertheless, they result in a correct expression in the semiclassical limit.

There have been many calculations of the tunneling propagator using the stationary phase approximation [24,26,27]. In these references the time evolution was allowed to be imaginary during the tunneling, but the wave properties were not completely included. These methods lead to results equivalent with the WKB approximation. We have managed to go beyond this approximation because our propagator gives the exact wave-function expression (38) for a monochromatic plane wave. As a matter of fact, in Appendix B we show that our propagator is exact when  $t_{fi} \rightarrow \infty$ .

## VI. PROPAGATOR FOR MORE GENERAL POTENTIAL BARRIERS

In principle the present treatment can be extended to more general potential barriers. The work by Miller and George [15–18] has shown how time-dependent trajectories can traverse classically forbidden regions. The method is, however, rather difficult to implement and requires extended numerical calculations. The imaginary time trajectories can be found only iteratively in order to reach the final coordinates  $(t_f, x_f)$ . When the potential can be divided into steep edges and nearly constant portions, our present semiclassical approach becomes an accurate and fast way to evaluate the tunneling propagator. When such a division of the potential is not possible, one cannot separate the wave and particle aspects as we have done. An example is the inverted parabolic barrier, as shown by Brink and Smilansky in Ref. [28].

When one wants to obtain a numerically accurate approximation to the tunneling propagator, one can use a step-function approximation for a potential of arbitrary shape. This was, to the best of our knowledge, first pointed out by Landauer [29]. We introduce the staircase approximation to the potential as shown in Fig. 6(A). At each step we use the wave mechanical transmission and reflection coefficients, and in the constant potential region we use semiclassical expressions for the trajectories. In this way we build up a branching tree series of semiclassical trajectories according to Fig. 6(B). When the number of steps is increased, the number of terms in this sum grows rapidly. However, we can sum over the branches, which gives recursion relations between transmission and reflection contribution of the  $n$ th step and preceding  $(n-1)$  steps. This means that if we divide the barrier into  $N$  steps, we obtain the transmission contribution after  $N$  recursion loops. The calculation is completely analytical and can be carried out rapidly and accurately.

When the potential rises steeply, the vertical parts of the steps become large and the wave properties dominate. Along slowly varying portions of the potential the horizontal parts can be extended, and the particlelike approximation to the propagator dominates. Thus the complementary interpretation of the approach retains its va-

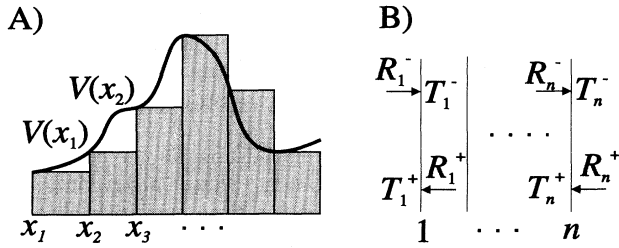


FIG. 6. A generic potential is discretized into piecewise constant parts (A). In the rightmost figure (B), only the boundaries are shown. The path can branch from each boundary due to reflection and transmission.

lidity even in the case of a general potential function.

The approximation of a potential barrier by a set of steps is, in fact, an accurate representation of many systems of physical interest. It is a good model for many semiconductor devices like double barriers, Josephson junctions, and infinite Bloch lattices. The consecutive interfaces can be used to split the semiclassical trajectories, which may be used to describe many properties in such devices. We believe that most such phenomena can be understood better by using classical concepts and a semiclassical interpretation of the tunneling.

Another problem occurs when we want to calculate the semiclassical trajectories in time-dependent potentials. A direct continuation of  $V(t)$  to complex times is questionable both from numerical and fundamental points of view. In fact, the propagation inside the barrier takes place along imaginary time (see Fig. 2), and we may surmise that this should not see a variation of the physical size of the barrier. We may try the separation of classical action in the interval  $t \in [t_-, t_- - i\tau]$  [see Eq. (13)] into static and negligible parts. With the potential

$$V(t) = V_0 + V_1(t), \quad (39)$$

this leads to

$$S = \int \left\{ \frac{1}{2} m \dot{x}^2 - [V_0 + V_1(t_-)] \right\} dt - \int [V_1(t) - V_1(t_-)] dt, \quad (40)$$

where we neglect the second contribution during propagation through the barrier. Thus the imaginary-time evolution takes place in the static potential  $V_0 + V_1(t_-)$ , where  $t_-$  is the time when the trajectory hits the edge of the potential. Up to that time, the classical paths are evaluated in the full potential  $V(t)$ ; the classical formalism in Secs. II and III allows this generalization directly. In our case,  $V=0$  for  $|x| > a$ , and the time dependence of the potential enters only through the value  $V_1(t_-)$ , where  $t_-$  depends on the previous history of the trajectory. As a result the propagator becomes the same as in Eq. (37), and the velocity  $v_i$  is obtained from Eqs. (17) and (36). Instead of result (9), the velocity  $w$  acquires a dependence on  $t_-$ :

$$w_2 = \left[ \frac{2[V_0 + V_1(t_-)]}{m} - v_i^2 \right]^{1/2}. \quad (41)$$

The replacement of  $V(t)$  by a static value can be considered as an adiabatic approximation. As the tunneling appears to take a negligible time compared with the real propagation of the wave packet, we may expect adiabatic conditions to prevail. In the complex time domain it is, however, difficult to justify this. The real proof is the numerical success of the method presented in Sec. VII.

## VII. NUMERICAL APPLICATIONS

We have applied the semiclassical path-summation method introduced in previous sections to time-dependent tunneling calculations. In these computations we have evolved the initial wave function according to integral (1), where we used the semiclassical propagator as the linear kernel. This gives the tunneled and reflected wave functions from which we have obtained the  $k$  representation of the wave function and the tunneling and reflection probabilities. In particular, we considered a constant rectangular potential, a simple double barrier, and a periodically modulated one. The results are compared with an exact numerical integration of the time-dependent Schrödinger equation using the split-operator method [13,21]; its application to wave-packet propagation is discussed in Ref. [21]. The semiclassical propagator method has been found to be accurate and fast. A typical run takes 1 min on the Convex C3840 computer.

In order to justify the use of a rectangular potential we choose the parameters corresponding to a heterostructure in GaAs [30,31]. The effective mass is thus taken to be  $m^* = 0.07m_e$ , the height of the barrier is taken to be  $V_0 = 0.23$  eV, and its width is 50 Å. The initial electronic wave packet is chosen to be Gaussian:

$$\Psi(x_i, t_i) = \left[ \frac{1}{2\pi\delta^2} \right]^{1/4} e^{-\frac{(x_i - x_0)^2}{4\delta^2}} e^{ik_0(x_i - x_0)}, \quad (42)$$

where the width is  $\delta = 500$  Å. This wave packet is broad enough to have a reasonably well-defined averaged momentum, and thus a well-defined energy. Thus its reflection and tunneling should be in good agreement with the steady-state plane-wave results, which are easily obtained.

The initial and final positions of the wave packet are chosen far away from the barrier  $x_f = |x_i| = 12\delta = 0.6$  μm. Figure 7 shows how the initial wave packet (upper part of Fig. 7) is divided into reflected and transmitted wave packets after encountering the barrier (lower part of Fig. 7). This picture is obtained by the use of the semiclassical propagator method, and we can see how the shape of the initial wave packet is preserved in both parts of the wave function after the interaction. This behavior is verified by direct integration of the Schrödinger equation. Because the incoming pulse has a narrow spread in energy, we can compare the reflection and transmission probabilities with steady-state results obtained from Eq. (38). This is carried out in Fig. 8 for a range of incoming energies. In part (A) the transmission probability  $T_{\text{prob}}$  is calculated from a semiclassically propagated wave packet

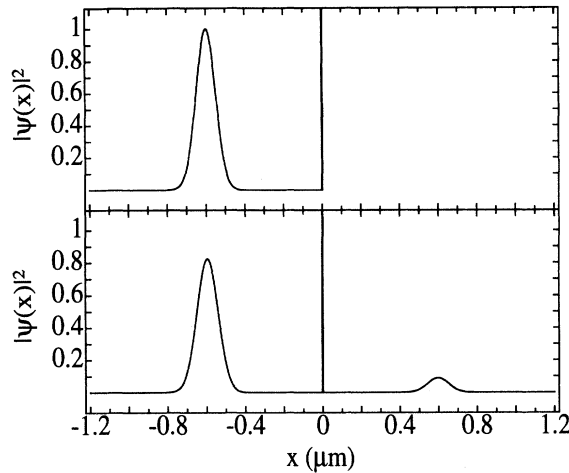


FIG. 7. The propagator method evolves an initial wave packet into reflected and transmitted wave functions. The mean energy of the initial wave packet is  $0.72V_0$ . The line at  $x=0$  denotes the position of the barrier.

and compared with the transmission probability of a monoenergetic wave function  $T_{\text{mono}} = \mathcal{T}^* \mathcal{T}$ . The results agree within our plotting accuracy, and hence we show the relative difference between the two results in part (B). As we can see, for this initial state the numerical difference remains better than 1%. To stress the wave mechanical aspects of our particle computation, we point out that for energies  $E > V_0$  the curve denotes over barrier transmission, when the branching of paths deriving from multiple reflections is necessary in order to obtain the correct result. These multiple reflections above the barrier have been summed in the steady state by Berry in Ref. [32] and by Holstein in Ref. [27].

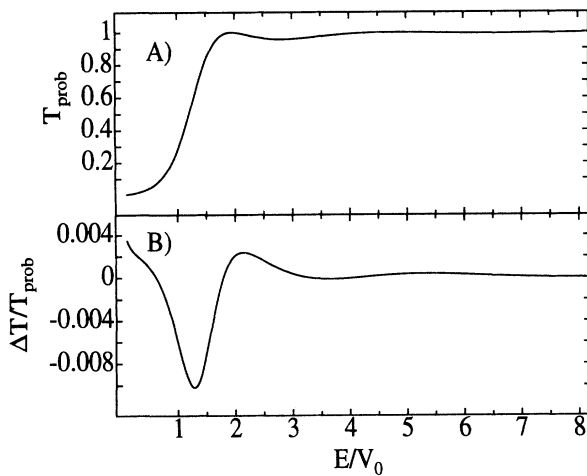


FIG. 8. Picture (A) illustrates the transmission probability  $T_{\text{prob}}$  of the static barrier calculated using the propagator method. The monochromatic result  $T_{\text{mono}} = \mathcal{T}^* \mathcal{T}$  is so close to this that only the relative difference  $\Delta T/T_{\text{prob}} = (T_{\text{prob}} - T_{\text{mono}})/T_{\text{prob}}$  is presented in picture (B).

To prove the utility of the staircase approximation to obtain numerically reliable results quickly, we have computed the tunneling in the double-barrier structure shown in Fig. 9. The potentials consist of two hyperbolic secant barriers of the form

$$V(x) = \frac{V_0}{\cosh^2(\alpha x)}, \quad (43)$$

where the parameters correspond to the case of GaAs (see above), and  $\alpha^{-1} = 20 \text{ \AA}$ . The two barriers are situated at a distance of  $100 \text{ \AA}$  apart. The lower part of Fig. 9 shows the computed tunneling probability obtained using a staircase approximation consisting of 500 steps of size  $0.8 \text{ \AA}$ . The accuracy of the result has been checked against the direct numerical integration of the time-dependent Schrödinger equation. For a single barrier only, the tunneling probability can be obtained analytically; the staircase approximation has been checked against this result as well. As in Fig. 8, the differences between the various approaches are well below 1% and thus not visible in the figure. It would be straightforward to use the time-dependent propagator to evolve an initial wave packet through the double-barrier structure, as in Fig. 7. These calculations prove the utility of the semiclassical approach as a tool for computations of results for arbitrary barriers.

When we add a periodic modulation to the height of the barrier, according to Eq. (40) we encounter additional phenomena. The imaginary velocity under the barrier has to be calculated from the static part  $V_0 + V_1(t_-)$  in Eq. (41). The incoming energy  $E_0$  is no longer conserved [33]. We can compare our results with those obtained by Büttiker and Landauer [9,34] if we set

$$V_1(t) = V_1 \sin \omega t. \quad (44)$$

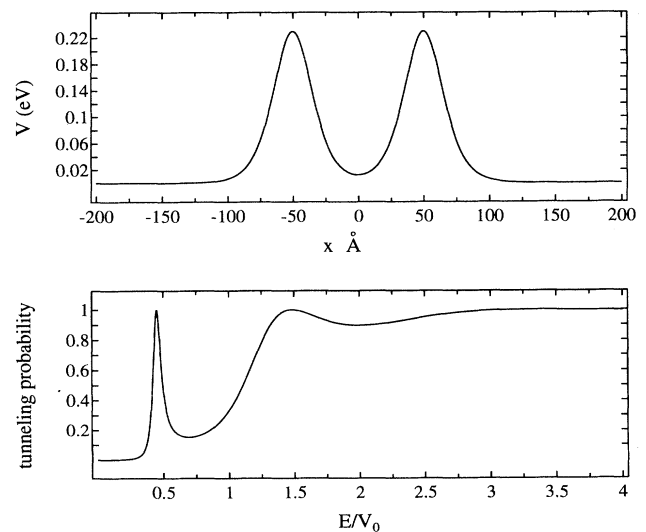


FIG. 9. A smooth double barrier is illustrated in the upper figure. The lower figure gives the transmission probability of the system calculated by dividing the barrier system into 500 equally spaced stepwise parts from  $-200$  to  $200 \text{ \AA}$ .

As expected, the energy of the transmitted wave packet acquires sidebands at multiples of the modulation frequency  $E_n = E_0 + n\hbar\omega$ . This derives from the fact that the barrier acts as a modulated nonlinear gate. We have found this effect both in the semiclassical propagator simulations and in the direct evaluation of the time-dependent solution of the Schrödinger equation.

In our calculations we choose  $V_1 = 0.05V_0$  and  $\hbar\omega = 0.35V_0$ . In Fig. 10 we compare the energy spectrum of the transmitted wave function using both the semiclassical propagator and the numerical computations. The energy is written directly using the equation

$$E_k = \frac{\hbar^2 k^2}{2m^*}, \quad (42)$$

and referred to the initial energy  $E_0 = 0.72V_0$  calculated from  $k_0$  in Eq. (42). To emphasize the agreement between the two calculations we use a logarithmic scale, and we can clearly see the periodic modulation with the energy difference  $\hbar\omega$  (this is indicated in the figure). The dotted curve is the numerical result, which shows two side peaks on each side of the main peak, and the rest of the peaks are lost in the numerical inaccuracy at the level  $10^{-8}$ . The solid line gives the result of the semiclassical propagator method. For the central peaks the results of the two calculations agree remarkably well. The semiclassical propagator method has a numerical error at level  $10^{-15}$  only, and hence we can see three more side peaks well resolved in the result of this calculation. Because of the asymptotic nature of the calculation, the method breaks down for low energies  $E \approx 0$ . Thus there is less of an agreement on the second sideband on the low-energy side. Büttiker and Landauer (BL) give an analytic expression for the first two side peaks,  $n = \pm 1$ . The amplitudes given by their theory are indicated as  $BL_{\pm}$  in Fig. 10; they are found to agree well with our results.

The calculations verify that the semiclassical path propagator contains all relevant physical information. In particular, we note that the tunneling imaginary-time paths are calculated using the static approximation of Eq. (41) (the adiabatic assumption). The close agreement with the wave-packet integration justifies *a posteriori* our neglect of time evolution during the imaginary-time in-

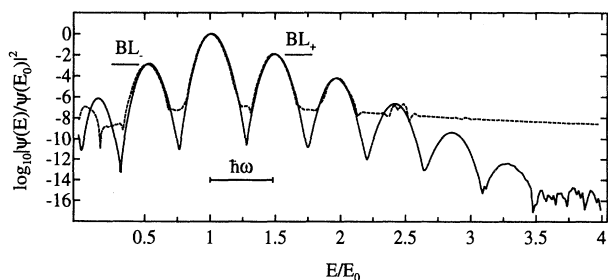


FIG. 10. The potential is subject to harmonic modulation. The energy representation of the tunneled wave function is shown. The solid curve is calculated using the propagator method, and the dashed curve using the split-operator method. The lines  $BL_-$  and  $BL_+$  illustrate the intensities of the first side peaks calculated from the Büttiker-Landauer theory.

tegration. The advantage of the use of semiclassical path summation is its shorter computational time and low numerical error level as compared with the split-operator method.

## VIII. CONCLUSIONS

We have introduced a semiclassical description of quantum-mechanical tunneling by extending the particle trajectories into the classically forbidden regions. In the spirit of Miller and George, we obtain these trajectories by integrating the classical equations of motion in the imaginary-time direction. Then the stationary phase approach giving the classical equations of motion has to be replaced by a method of steepest descent. It is, however, not possible to neglect the wave character of quantum particles completely, if accurate numerical results are desired. At interfaces between allowed and forbidden regions, the semiclassical trajectories branch, and the branching ratio must be obtained from wave calculations. We consider this to be an essential manifestation of the complementary nature of quantum time evolution. The repeated branching of the semiclassical paths attaches to any individual one a whole family of related paths which arise from repeated reflections at the interfaces.

When all the families of semiclassical paths are summed in a path-summation representation of the quantum propagator, we can obtain an asymptotically accurate description of the tunneling phenomenon. This is verified on the transmission of a wave packet across a rectangular barrier. The semiclassical result is compared, on the one hand, with the pure wave result for the transmission probability (Fig. 8), and on the other hand with a direct numerical solution of the Schrödinger equation. Excellent agreement is found. We have also shown that the semiclassical results can be used as an approximate method to treat numerically an arbitrary potential structure.

We have also tested the method in the case of a periodically modulated barrier. This case has been treated earlier by other researchers, and we consider it an interesting test case for the range of validity of our approach. Utilizing a simple adiabatic approximation, we find (cf. Fig. 10) that we obtain excellent results using less computer time and achieving higher accuracy than the direct integration method. Thus we recommend our method for a wide variety of physical situations, even if we cannot assert the exact range of situations where it may be useful. As a first attempt at investigating a particular situation, it should offer a cheap and fast way to obtain results.

From a strict formal point of view, the tunneling occurs in imaginary time and no real-time delay is introduced. The wave function starts to appear on the far side of the barrier as soon as it hits the near edge. When tunneling times are part of some measurable observable, there will appear an unavoidable delay. The exact value of this depends on the manner of observing the delay. In a forthcoming paper, we plan to discuss the various manifestations of tunneling delay times, and try to elucidate their properties by applying the presently introduced method of semiclassical paths.

## ACKNOWLEDGMENTS

We want to thank Professor T. F. George for invaluable discussion of the imaginary-time method and for valuable encouragement over many years. We also thank Dr. O. Tirkkonen for fruitful discussions about the path-integral method. We are grateful to the Center of Scientific Computation (CSC) for making their supercomputer facilities available for our research project. Our project is supported by the Academy of Finland and the Väisälä foundation.

## APPENDIX A

Here we prove that coefficient  $A^{(n)}$  in Eq. (18) varies more slowly than the term with the classical action in the exponential. The coefficient  $A^{(n)}$  can be obtained from the quantum correction path integral in Eq. (4):

$$A^{(n)}(v_i, t_i, t_f) = \int \mathcal{D}\eta e^{i\tilde{S}^{(n)}(\tilde{\eta}, \eta, x_{cl})}. \quad (\text{A1})$$

Generally  $t_f$  has also an imaginary part and the integration is performed along a contour similar to that in Fig. 2. The quantum excursions  $\eta$  are zero at both initial and final times. The form of the path integral suggests that  $A^{(n)}$  depends on  $x_f$  and  $x_i$  only through the classical path  $x_{cl}$  which is determined uniquely by the initial velocity. Thus  $A^{(n)}$  is a function of  $t_i$ ,  $t_f$ , and  $v_i$ . Next we take the derivative of the propagator, just as in Eq. (20):

$$\begin{aligned} \frac{\partial K}{\partial x_f} &= \frac{i}{\hbar} \frac{\partial S_{cl}^{(n)}}{\partial x_f} e^{iS_{cl}^{(n)}/\hbar} A^{(n)} + e^{iS_{cl}^{(n)}/\hbar} \frac{\partial v_i}{\partial x_f} \frac{\partial A^{(n)}}{\partial v_i} \\ &= e^{iS_{cl}^{(n)}/\hbar} \left[ \frac{i}{\hbar} m v_f A^{(n)} \pm \frac{1}{t_{\tilde{\eta}}} \frac{\partial A^{(n)}}{\partial v_i} \right] \\ &= \frac{i}{\hbar} m v_f e^{iS_{cl}^{(n)}/\hbar} A^{(n)} \left[ 1 \pm \frac{1}{t_{\tilde{\eta}}} \frac{\hbar}{i m v_f} \frac{1}{A^{(n)}} \frac{\partial A^{(n)}}{\partial v_i} \right], \end{aligned} \quad (\text{A2})$$

where Eqs. (17) and (20) have been used: the plus and minus signs come from the absolute value of  $x_f$  in Eq. (17). Assume that we investigate a chosen event after the reflection or the tunneling. This means that we have to keep  $v_i$  constant as we increase  $t_{\tilde{\eta}}$  because the particle is free after encountering the barrier. Consequently only the free propagation is added to the propagator, and the quantum correction  $A^{(n)}$  behaves as in the free-particle case. This means that the derivative term

$$\frac{\hbar}{i m v_f} \frac{1}{A^{(n)}} \frac{\partial A^{(n)}}{\partial v_i} \quad (\text{A3})$$

does not depend on  $t_{\tilde{\eta}}$  assuming that  $v_i$  is kept constant.

Thus in the asymptotic limit  $t_{\tilde{\eta}} \rightarrow \infty$  ( $v_i$  is kept constant) the second term in (A2) vanishes, and only the classical action term contributes to Eq. (A2). This result also means that, inside an integral like Eq. (1),  $A^{(n)}$  can be treated as a constant because it varies more slowly than the term with the classical action in the exponential.

Next we check how large  $t_{\tilde{\eta}}$  should be in order to justify the asymptotic limit. For example, for  $A^{(0)}$  from Eqs. (33) and (34), we obtain

$$\begin{aligned} A^{(0)} &\approx \left[ \frac{m}{2\pi i \hbar t_{\tilde{\eta}}} \right]^{1/2} T_- T_+ \\ &= \left[ \frac{m}{2\pi i \hbar t_{\tilde{\eta}}} \right]^{1/2} \frac{4i v_i w}{(v_i + i w)^2}. \end{aligned} \quad (\text{A4})$$

Expression (A3) becomes

$$\frac{\hbar}{i m v_f} \frac{1}{A^{(0)}} \frac{\partial A^{(0)}}{\partial v_i} = \frac{\hbar}{m} \left[ \frac{v_i - i w}{v_i w} \right]^2. \quad (\text{A5})$$

This is independent of  $t_{\tilde{\eta}}$  because  $v_i$  is constant, as mentioned above. For typical numerical parameters, the absolute value of the additional term in the expression (A2) becomes  $5 \times 10^{-3}$  times the major term. This justifies the use of the asymptotic expressions in the numerical calculations.

## APPENDIX B

In this appendix we show that the constant energy propagator derived by de Aguiar agrees with our result in the limit that  $t_{\tilde{\eta}} \rightarrow \infty$ . De Aguiar derived an exact expression for the space-energy representation of the propagator (Green function) for the rectangular potential [19]. The connection to the space-time representation is obtained by the Fourier transformation

$$\begin{aligned} K(x_f, x_i; t_{\tilde{\eta}}) &= \frac{i}{2\pi} \int_0^\infty DK(x_f, x_i; E) e^{-iEt_{\tilde{\eta}}/\hbar} dE \\ &= \frac{i}{2\pi} \int_{-\infty}^\infty K(x_f, x_i; E_k) \\ &\quad \times e^{-iE_k t_{\tilde{\eta}}/\hbar} \frac{\hbar^2}{m} k dk, \end{aligned} \quad (\text{B1})$$

where we have changed the  $E$  integration to a  $k$  integration by the substitution  $E_k = \hbar^2 k^2 / 2m$ . Following the notations of Ref. [19],  $DK = K^+ - K^-$  consists of the retarded and advanced Green functions. The Green function  $K(E)$  in the last term of Eq. (B1) will be determined below. The imaginary prefactor in (B1) is chosen in such a way that the notation in our paper agrees with those of Ref. [19]. Next we pick up those terms from de Aguiar's results corresponding to Eq. (37):

$$\begin{aligned} K(x_f, x_i; E) &= \frac{m}{ik\hbar^2} [e^{ik|x_f - x_i|} + \mathcal{R}(k)e^{-ik(x_f + x_i + 2a)}] \Theta(-x_f - a) + \frac{m}{ik\hbar^2} \mathcal{T}(k)e^{ik(x_f - x_i - 2a)} \Theta(x_f - a) \\ &= \frac{m}{ik\hbar^2} [e^{ikv_i t_{\tilde{\eta}}} + \mathcal{R}(k)e^{ikv_i t_{\tilde{\eta}}}] \Theta(-x_f - a) + \frac{m}{ik\hbar^2} \mathcal{T}(k)e^{ikv_i t_{\tilde{\eta}}} \Theta(x_f - a), \end{aligned} \quad (\text{B2})$$

where we have applied the velocity relations (17) and (36). Furthermore, the initial position is assumed to be left of the barrier  $x_i \leq a$ . By using Eqs. (B1) and (B2) we obtain the space-time propagator

$$\begin{aligned}
K(x_f, x_i; t_{\hbar}) &= \frac{1}{2\pi} \int_{-\infty}^{\infty} [e^{ikv_i t} + \mathcal{R}(k)e^{ikv_i t}] e^{-i\hbar k^2 t/2m} dk \Theta(-x_f - a) + \frac{1}{2\pi} \int_{-\infty}^{\infty} \mathcal{T}(k) e^{ikv_i t} e^{-i\hbar k^2 t/2m} dk \Theta(x_f - a) \\
&= \frac{1}{2\pi} \left[ e^{im(v_i^d)^2 t/2\hbar} \int_{-\infty}^{\infty} e^{-i(k - mv_i^d/\hbar)^2 \hbar t/2m} dk + e^{imv_i^2 t/2\hbar} \int_{-\infty}^{\infty} \mathcal{R}(k) e^{-i(k - mv_i/\hbar)^2 \hbar t/2m} dk \right] \Theta(-x_f - a) \\
&\quad + \frac{1}{2\pi} \left[ e^{imv_i^2 t/2\hbar} \int_{-\infty}^{\infty} \mathcal{T}(k) e^{-i(k - mv_i/\hbar)^2 \hbar t/2m} dk \right] \Theta(x_f - a) \\
&= \Theta(-x_f - a) \left[ K_{\text{cl}}^d \left[ \frac{i\hbar t}{2\pi m} \right]^{1/2} \int_{-\infty}^{\infty} e^{-iu^2 \hbar t/2m} du + K_{\text{cl}} \left[ \frac{i\hbar t}{2\pi m} \right]^{1/2} \int_{-\infty}^{\infty} \mathcal{R}(u + mv_i/\hbar) e^{-iu^2 \hbar t/2m} du \right] \\
&\quad + K_{\text{cl}} \left[ \frac{i\hbar t}{2\pi m} \right]^{1/2} \int_{-\infty}^{\infty} \mathcal{T}(u + mv_i/\hbar) e^{-iu^2 \hbar t/2m} du \Theta(x_f - a), \tag{B3}
\end{aligned}$$

where we have used the classical propagator expression (33) and changed the integration variable to  $u = k - mv_i/\hbar$ . The first integral term in (B3) becomes

$$\begin{aligned}
\left[ \frac{i\hbar t}{2\pi m} \right]^{1/2} \int_{-\infty}^{\infty} e^{-iu^2 \hbar t/2m} du \\
= \left[ \frac{i\hbar t}{2\pi m} \right]^{1/2} \left[ \frac{2\pi m}{i\hbar t} \right]^{1/2} = 1. \tag{B4}
\end{aligned}$$

The integration which contains  $\mathcal{T}$  or  $\mathcal{R}$  cannot be evaluated analytically. However, in the asymptotic limit  $t_{\hbar} \rightarrow \infty$  the exponential term in the integral in Eq. (B3)

oscillates rapidly as  $u$  increases. Hence the integral contributes only near  $u=0$ . This means that  $\mathcal{T}$  and  $\mathcal{R}$  can be taken as constant in the integration (B3), which thus gives the same value as (B4). Now we can rewrite Eq. (B3) as

$$\begin{aligned}
K(x_f, x_i; t_{\hbar}) &= [K_{\text{cl}}^d + K_{\text{cl}} \mathcal{R}(mv_i/\hbar)] \Theta(-a - x_f) \\
&\quad + K_{\text{cl}} \mathcal{T}(mv_i/\hbar) \Theta(x_f - a), \tag{B5}
\end{aligned}$$

which is the same as Eq. (37). We conclude that for a rectangular potential barrier, the semiclassical propagator derived in this paper becomes asymptotically exact in the limit  $t_{\hbar} \rightarrow \infty$ .

- 
- [1] C. Weissbuch and B. Vinter, *Quantum Semiconductor Structures* (Academic, New York, 1991).
- [2] E. Merzbacher, *Quantum Mechanics* (Wiley, New York, 1961).
- [3] L. S. Schulmann, *Technics and Applications of Path Integrals* (Wiley, New York, 1981).
- [4] S. Coleman, in *The Whys of Subnuclear Physics, Erice Lectures 1977*, edited by A. Zichicki (Plenum, New York, 1979).
- [5] A. O. Caldeira and A. J. Leggett, *Ann. Phys. (N.Y.)* **140**, 118 (1983).
- [6] Several review articles in *Phys. Today* **43** (5), 23 (1990).
- [7] A. P. Jauho, in *Hot Carriers in Semiconductor Nanostructures: Physics and Applications*, edited by J. Shan (Academic, New York, 1992), p. 121.
- [8] E. H. Hauge and J. A. Stovng, *Rev. Mod. Phys.* **61**, 917 (1989).
- [9] M. Buttiker and R. Landauer, *Phys. Rev. Lett.* **49**, 1739 (1982).
- [10] X. Jiang, *J. Phys. Condens. Matter* **2**, 6553 (1990).
- [11] A. D. Stone, M. Y. Azbel, and P. A. Lee, *Phys. Rev. B* **31**, 1707 (1985).
- [12] A. P. Jauho, *Phys. Rev. B* **41**, 12 328 (1990).
- [13] M. F. Bjrksten, R. M. Nieminen, and K. Laasonen, *J. Phys. Condens. Matter* **3**, 7007 (1991).
- [14] M. S. Child, *Molecular Collision Theory* (Academic, New York, 1974).
- [15] W. H. Miller and T. F. George, *J. Chem. Phys.* **56**, 5637 (1972).
- [16] W. H. Miller and T. F. George, *J. Chem. Phys.* **56**, 5668 (1972).
- [17] W. H. Miller and T. F. George, *J. Chem. Phys.* **57**, 5019 (1972).
- [18] T. F. George and W. H. Miller, *J. Chem. Phys.* **57**, 2458 (1972).
- [19] M. A. M. de Aguiar, *Phys. Rev. A* **48**, 2567 (1993).
- [20] T. O. de Carvalho, *Phys. Rev. A* **47**, 2562 (1993).
- [21] K. A. Suominen, B. Garraway, and S. Stenholm, *Phys. Rev. A* **45**, 3060 (1992).
- [22] R. P. Feynman and A. R. Hibbs, *Quantum Mechanics and Path Integrals* (McGraw-Hill, New York, 1965).
- [23] B. I. Ivlev and V. I. Mel'nikov, *Phys. Rev. Lett.* **55**, 1614 (1985).
- [24] D. W. McLaughlin, *J. Math. Phys.* **13**, 1099 (1972).
- [25] J. R. Reitz, F. J. Milford, and R. W. Christy, *Foundations of Electromagnetic Theory* (Addison-Wesley, London, 1980).
- [26] B. R. Holstein and A. R. Swift, *Am. J. Phys.* **50**, 833 (1982).
- [27] B. R. Holstein, *Am. J. Phys.* **52**, 321 (1984).
- [28] D. M. Brink and U. Smilansky, *Nucl. Phys. A* **405**, 301 (1983).

- [29] R. Landauer, *Phys. Rev.* **82**, 80 (1951).
- [30] P. E. Lindelof, *Lectures at Summer School on Nanometer Structures and Mesoscopic Physics, Trondheim, Norway, 1992* (unpublished).
- [31] A. P. Jauho and M. Johnson, *J. Phys. Condens. Matter* **1**, 9027 (1989).
- [32] M. Berry, *J. Phys. A* **15**, 3693 (1982).
- [33] M. Kleber, *Phys. Rep.* **237**, 331 (1994).
- [34] M. Büttker and R. Landauer, *Phys. Scr.* **32**, 429 (1985).